JEM

Brief Definitive Report

Contextual control of skin immunity and inflammation by *Corynebacterium*

Vanessa K. Ridaura,[1]* Nicolas Bouladoux,[1,2]* Jan Claesen,[4] Y. Erin Chen,[4] Allyson L. Byrd,[1,3,5] Michael G. Constantinides,[1] Eric D. Merrill,[1] Samira Tamoutounour,[1] Michael A. Fischbach,[4] and Yasmine Belkaid[1,2]

[1]Mucosal Immunology Section, Laboratory of Parasitic Diseases and [2]Microbiome Program, National Institute of Allergy and Infectious Diseases, National Institutes of Health, Bethesda, MD
[3]Translational and Functional Genomics Branch, National Human Genome Research Institute, National Institutes of Health, Bethesda, MD
[4]Department of Bioengineering, Stanford University, Stanford, CA
[5]Department of Bioinformatics, Boston University, Boston, MA

How defined microbes influence the skin immune system remains poorly understood. Here we demonstrate that *Corynebacteria*, dominant members of the skin microbiota, promote a dramatic increase in the number and activation of a defined subset of γδ T cells. This effect is long-lasting, occurs independently of other microbes, and is, in part, mediated by interleukin (IL)-23. Under steady-state conditions, the impact of *Corynebacterium* is discrete and noninflammatory. However, when applied to the skin of a host fed a high-fat diet, *Corynebacterium accolens* alone promotes inflammation in an IL-23–dependent manner. Such effect is highly conserved among species of *Corynebacterium* and dependent on the expression of a dominant component of the cell envelope, mycolic acid. Our data uncover a mode of communication between the immune system and a dominant genus of the skin microbiota and reveal that the functional impact of canonical skin microbial determinants is contextually controlled by the inflammatory and metabolic state of the host.

INTRODUCTION

The skin is the body's most exposed interface with the environment and acts as a first line of physical and immunological defense. This organ is also a complex and dynamic ecosystem inhabited by a multitude of microorganisms (Belkaid and Segre, 2014). These microbes play a fundamental role in the control of skin physiology, including skin immunity and inflammatory processes (Lai et al., 2009; Naik et al., 2012). However, despite the formidable diversity of skin microbes, thus far only a handful of specific microbes and microbe-associated molecules have been linked to defined immunological or inflammatory processes. Although little is known about the mechanisms by which skin microbes influence the skin immune system at steady state, even less is known about how this dialog is altered under conditions of inflammation. Identifying dominant microbe-derived immune modulators and the context controlling the impact of these microbes on the immune system may help us understand the association between defined members of the skin microbiota and the skin immune system under both steady-state and disease settings.

Here, we demonstrate that members of a dominant bacterial genus of the skin, *Corynebacterium*, promote IL-23–dependent responses under steady-state and inflammatory conditions and reveal that expression of a major component of the *Corynebacterium* cell wall, mycolic acid, is required to mediate these responses. Further, we show that the impact of microbial determinants on tissue immunity can be highly controlled by the inflammatory and metabolic status of the host.

RESULTS AND DISCUSSION

Distinct effect of *Corynebacterium accolens* on dermal γδ TCR^{low} IL-17A^{+} (γδ T17) cells

To uncover novel microbial species or microbiota-derived molecules that engage the skin immune system, we developed a generalizable culturing approach to isolate microbial taxa from the skin of WT mice, from the skin of mice with defined immune deficiencies, or from skin swabs collected from healthy human volunteers. We used both a classical (αβ TCR^{+}) and nonclassical (γδ TCR^{+}) skin lymphocyte cytokine potential profile as the read-out of an in vivo screen. Specific pathogen-free (SPF) animals, raised under conventional settings (with an endogenous microbiota), were topically associated with distinct bacteria. At 14 d after the initial microbial application, skin T cell subset frequency and cytokine potential profiles were assessed (Fig. 1 A and Fig. S1, A and B).

*V.K. Ridaura and N. Bouladoux contributed equally to this paper.

Correspondence to Yasmine Belkaid: ybelkaid@niaid.nih.gov; Michael A. Fischbach: fischbach@fischbachgroup.org

J. Claesen's present address is Dept. of Cellular and Molecular Medicine, Lerner Research Institute, Cleveland Clinic, Cleveland, OH.

V.K. Ridaura's present address is Verily Life Sciences, South San Francisco, CA.

The Rockefeller University Press
J. Exp. Med. 2018 Vol. 215 No. 3 785–799
https://doi.org/10.1084/jem.20171079

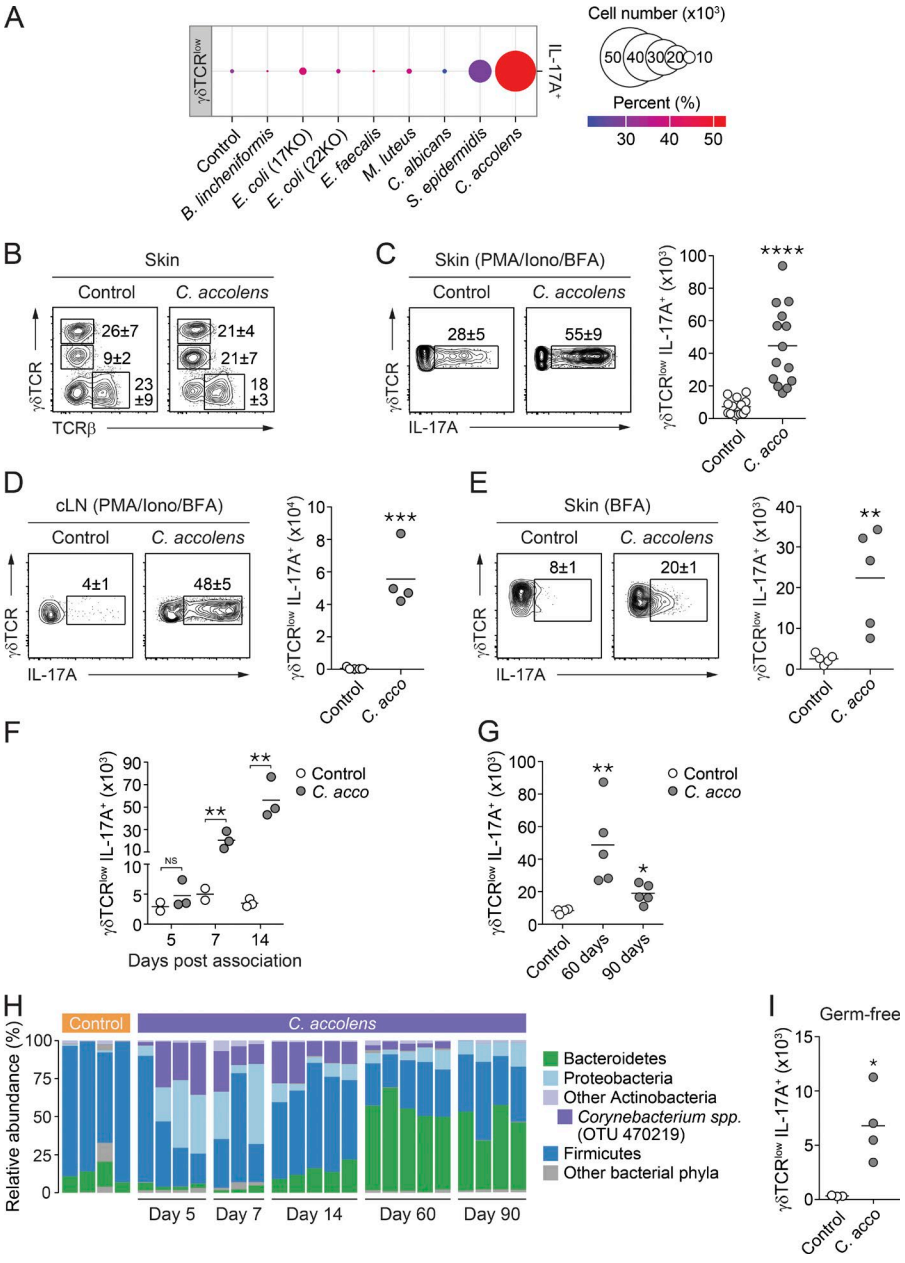

Figure 1. **Dermal γδ T17 cells increase upon cutaneous *C. accolens* association. (A)** Mean of absolute numbers (represented by the size of the circles) and frequencies (represented by the colors of the circles) of IL-17A–producing CD45$^+$ CD90.2$^+$ γδ TCR^{low} cells in the skin of mice previously associated or not with distinct skin commensal microbes. Data were collected after in vitro restimulation with PMA and ionomycin (Iono) in the presence of BFA. Results are representative of three independent experiments with four to six animals per group. **(B)** Frequencies (mean ± SEM) of CD45$^+$ CD90.2$^+$ TCRβ$^+$ and γδ TCR^{low} cells from the skin of *C. accolens*–associated mice. **(C–E)** Frequencies (mean ± SEM) and absolute numbers of CD45$^+$ CD90.2$^+$ γδ TCR^{low} cells producing IL-17A in the skin (C) and ear-skin draining lymph nodes (cLN) (D) upon PMA/Iono restimulation in the presence of BFA or in the skin after treatment with BFA during tissue digestion (E). In B–E, data shown are representative of three independent experiments with three to eight mice per treatment group. **, $P < 0.01$; ***, $P < 0.001$; ****, $P < 0.0001$ as calculated by two-tailed, unpaired Student's *t* test. **(F and G)** Absolute numbers of γδ TCR^{low} IL-17A$^+$ cells (PMA/Iono restimulation in the presence of BFA) isolated from the ear skin of mice at different time points after the initial association. Data shown are representative of two independent experiments, with two to five animals per group. *, $P < 0.05$; **, $P < 0.01$ as calculated using one-way ANOVA with Holm-Šídák's multiple comparison test. **(H)** Relative abundance of skin associated microbiota from either naive control or *C. accolens*–associated animals at different days after the initial association, as determined by 16S rRNA gene sequencing of V1-V3 hypervariable regions. Each bar represents the percentage of sequences in operational taxonomic units assigned to each phylum for an individual mouse. Data shown are representative of two independent experiments, with three to five animals per group. **(I)** Absolute numbers of IL-17A–producing γδ TCR^{low} cells from the skin of unassociated control or *C. accolens*–mono-associated GF mice. Data collected after in vitro restimulation with PMA/Iono in the presence of BFA. Data shown are representative of two independent experiments, with three to four animals per group. *, $P < 0.05$ as calculated by two-tailed, unpaired Student's *t* test.

Notably, *C. accolens* had a particularly strong impact on the accumulation of IL-17A–producing γδ TCR^{low} T cells (Fig. 1, A–E; and Fig. S1 B), a population of migratory γδ T cells (γδ TCR^{low}) found in the mouse dermis (Cai et al., 2011). *Corynebacterium* is one of the three most abundant bacterial genera on human skin, found especially in moist sites (Grice et al., 2009). *Corynebacterium* species are also common members of the mouse skin microbiota (Grice et al., 2009; Belheouane et al., 2017). Given their prevalence, remarkably little is known about the effects of *Corynebacterium* on host immunity. After *C. accolens* association of mice previously devoid of *Corynebacterium* (Fig. 1 H), the frequency and absolute number of γδ TCR^{low} cells as well as their potential to produce IL-17A (γδ T17) were significantly increased in the skin and skin draining lymph node compared with unassociated controls (Fig. 1, B–E). Addition of brefeldin A (BFA) during tissue digestion revealed that, in contrast to cells from control mice, γδ TCR^{low} cells actively released

IL-17A after *C. accolens* association (Fig. 1 E). The impact on the γδ T17 cell number was detectable by 7 d after association and was durable, lasting up to 90 d after association (Fig. 1, F and G). The increase of γδ T17 cells in the skin of associated mice was uncoupled from inflammation as indicated by a lack of neutrophils and inflammatory monocyte recruitment and a lack of keratinocyte hyperplasia (Fig. S1, C–F). Such a response occurred even when bacteria were applied at doses as low as 10^6 CFU/cm^2 (Fig. S1, H and I) corresponding to the proposed biomass of skin commensals in humans (Grice and Segre, 2011). 16S ribosomal RNA (rRNA) gene sequencing of the skin-resident microbiota of associated and control mice confirmed that *C. accolens* was able to colonize the mouse skin in a durable manner and was associated with some changes to the structure of the resulting skin-associated microbiota, namely, an increase in Proteobacteria and a corresponding decrease in Bacteroidetes (Fig. 1 H). Colony-forming unit assessment confirmed that a low number of *C. accolens* was found on the skin of associated mice (Fig. S1, G and H). We next addressed if the impact of *C. accolens* was direct or dependent on *Corynebacterium*-induced changes in the endogenous community. As previously shown (Naik et al., 2015), mice raised in the absence of live microbes (germ-free [GF]) had a severe defect in IL-17A production by γδ T cells (Fig. 1 I). Monocolonization of GF animals with *C. accolens* resulted in a significant increase in γδ T17 cells within the skin revealing that the effect of *C. accolens* on γδ T cells was dominant and independent of other members of the cutaneous microbiota (Fig. 1 I).

The majority of γδ T17 cells after *C. accolens* association are activated Vγ4$^+$ dermal γδ T cells

At steady state, approximately half of the IL-17A–expressing γδ TCR^{low} cells also express Vγ4, whereas the remaining fraction is enriched in Vγ6 usage (Heilig and Tonegawa, 1986). Skin association with *C. accolens* resulted in the specific increase and activation of the Vγ4$^+$ subset of γδ T cells (Fig. 2, A–C). This contrasted with *Staphylococcus epidermidis*, which preferentially enhanced Vγ4-negative T cells (Fig. 2, A–C). Mice lacking the Vγ4$^+$ subset of γδ T cells (Gray et al., 2013) did not mount a compensatory Vγ4^{neg} response (Fig. 2 D). IL-17A–producing γδ T cells within the skin also expressed the chemokine receptor CCR6, allowing us to use this marker to isolate Vγ4$^+$ γδ T17 cells (Fig. 2 A). We sorted Vγ4$^+$ γδ TCR^{low} CCR6$^+$ cells from the skin of mice that had been associated for 14 d with either *C. accolens* or *S. epidermidis* or from unassociated controls and performed gene expression analysis using a NanoString chip designed to capture activation-associated lymphocyte gene expression (Table S1). Of note, gene-level expression for the IL-23 receptor was high in Vγ4$^+$ γδ TCR^{low} CCR6$^+$ cells under steady-state conditions (Fig. 2 E). Furthermore, expression of CCR4, a chemokine receptor linked to skin homing, was up-regulated in Vγ4$^+$ γδ TCR^{low} CCR6$^+$ cells collected from *C. accolens*–associated mice when compared with unassociated controls. Additionally, and in contrast to cells isolated from *S. epidermidis*–associated mice, gene-level expression of markers of T cell activation, such as TNFRSF4 (OX40), CD279 (PD-1), and STAT5, were also up-regulated (Fig. 2 E). Collectively, these results support the idea that *C. accolens* preferentially promoted the activation of Vγ4$^+$ γδ T cells.

γδ T17 induction is dependent on a phylogenetically conserved component of the cell envelope of *Corynebacterium* species

Numerous *Corynebacterium* species are common members of both mouse and human skin microbiota (Grice and Segre, 2011; Belheouane et al., 2017). To test if the ability to induce γδ T17 cells was a general feature of the *Corynebacterium* genus, we associated WT mice with nine different species of *Corynebacterium*. Notably, eight of the nine species induced a robust Vγ4$^+$ γδ T17 response (Fig. 3, A and B), supporting the idea that such a response was likely the result of a conserved feature among the species tested. One characteristic that distinguishes Corynebacteria from other gram-positive bacteria is an external lipid bilayer of all-carbon, branched fatty acids called mycolic acids, which forms a structure similar in size and location to the gram-negative outer membrane (Fig. 3 C) (Dörner et al., 2009). Interestingly, *C. amycolatum*, a rare *Corynebacterium* species that does not contain mycolic acids (Barreau et al., 1993), was the only *Corynebacterium* tested that failed to induce γδ T17 cells (Fig. 3, A and B).

To assess if mycolic acids or elements from the characteristic *Corynebacterium* cell envelope contributed to the Vγ4$^+$ γδ T17 expansion, we generated a mutant strain of *C. accolens* with a deletion in the mycolic acid synthase gene (Δ0503). In contrast to WT *C. accolens*, association of SPF mice with the mycolic acid–deficient strain Δ0503 did not induce Vγ4$^+$ γδ T17 within the skin compartment (Fig. 3, D and E). Because a defect in the cell envelope could potentially lead to defects in colonization efficacy, we monocolonized GF mice using the mutant or WT strains of *C. accolens*. Under these conditions, *C. accolens* Δ0503 also failed to induce a γδ T17 response compared with the WT strain (Fig. 3 F). To further confirm the involvement of the *Corynebacterium* cell envelope, we used an in vitro approach in which purified Vγ4$^+$ CCR6$^+$ T cells from the skin and regional LN of *C. accolens*–associated animals were restimulated ex vivo. Vγ4$^+$ CCR6$^+$ T cells from *C. accolens*–associated mice did not respond to heat-killed (hk) *C. accolens* bacteria alone, supporting the idea that this response was not associated with direct engagement of the γδ T cells by a microbially derived element (Fig. 3 G). On the other hand, and in contrast to unloaded splenic DCs, DCs loaded with hk *C. accolens* cells were able to promote the production of IL-17A by Vγ4$^+$ CCR6$^+$ T cells (Fig. 3 G).

Further confirming a role for mycolic acid expression, DCs loaded with hk Δ0503 *C. accolens* or hk *C. amyco-*

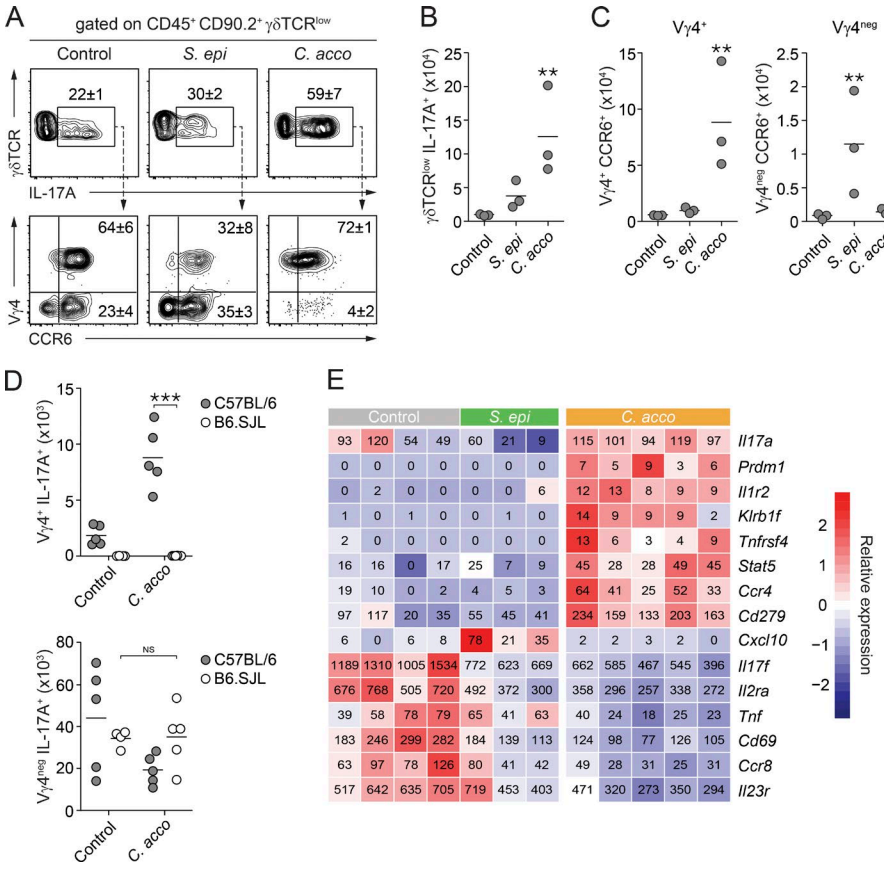

Figure 2. ***C. accolens* preferentially promotes the activation of Vγ4⁺ γδ T cells.** Mice were topically associated with *S. epidermidis* (*S. epi*) or *C. accolens* (*C. acco*) or left unassociated (Control). **(A)** Frequencies of skin CD45⁺ CD90.2⁺ γδ TCR^{low} cells producing IL-17A (top) and flow cytometric analysis of TCR Vγ4 (Vγ4) and CCR6 expression by those cells (bottom) 14 d after the first association. Numbers are mean frequencies (±SEM). **(B and C)** Absolute numbers of skin γδ TCR^{low} IL-17A⁺ (B), γδ TCR^{low}IL-17A⁺Vγ4⁺ CCR6⁺, and γδ TCR^{low} IL-17A⁺ Vγ4^{neg} CCR6⁺ (C) cells 14 d after the first association. In A–C, data shown are representative of two independent experiments with three animals per treatment group. **, P < 0.01 as calculated using one-way ANOVA with Holm-Šídák's multiple comparison test. **(D)** Absolute number of IL-17A–producing γδ TCR^{low} Vγ4⁺ and γδ TCR^{low} Vγ4^{neg} in the skin of unassociated or *C. accolens*–associated C57BL/6 or B6.SJL (Sox13-deficient) mice 14 d after the first association (n = 4–5 mice per group). Data shown are representative of two independent experiments. ***, P < 0.001; NS, not significant (one-way ANOVA with Holm-Šídák's multiple comparison test). **(E)** Heat map of relative gene expression analyzed by NanoString in γδ TCR^{low} Vγ4⁺ CCR6⁺ purified from unassociated control mice (Control, n = 4) or mice associated with *S. epidermidis* (*S. epi*, n = 3) or *C. accolens* (*C. acco*, n = 5; day 14 after association). Relative gene expression is clustered by sample (columns) and genes (rows) using Euclidean distance-based hierarchical clustering. Genes illustrated were significantly different after a two-way ANOVA with Tukey's correction for multiple hypotheses.

latum failed to promote IL-17A production from purified Vγ4⁺ CCR6⁺ cells (Fig. 3 G). To further test the contribution of the elements of the *Corynebacterium* cell envelope to Vγ4⁺ γδ T17 cell induction/activation, we isolated total envelope extracts (TEEs) from WT *C. accolens* bacteria and included this fraction in liposomes. DCs loaded with liposomes carrying TEE but not empty liposomes were able to stimulate IL-17A production from purified Vγ4⁺ CCR6⁺ cells (Fig. 3 G). In contrast, DCs loaded with lipoarabinomannans (LAMs), which are also present in the outer surface material of these *Corynebacteria* (Burkovski, 2013), were unable to induce IL-17A production by Vγ4⁺ γδ T cells (Fig. 3 G). Accordingly, DCs loaded with hk cells from a mutant strain of *C. striatum* (Δ647) bearing a deletion in a key LAM synthesis enzyme were still able to promote the production of IL-17 by Vγ4⁺ CCR6⁺ T cells (Fig. 3 G). Thus, the ability of *Corynebacterium* to activate γδ T cells in vitro is dependent on a cell envelope containing mycolic acid but not LAMs. Together, these results support the idea that mycolic acid (directly or via its ability to anchor a defined molecular determinant) plays a crucial role in the ability of *Corynebacterium* to activate Vγ4⁺ γδ T cells.

IL-23 plays a prominent role in mediating the effect of *C. accolens* on skin immunity

γδ T cells can be activated via distinct mechanisms, including antigen-specific stimulation and various innate mechanisms, such as direct responses to inflammatory cytokines (Sutton et al., 2009; Vantourout and Hayday, 2013). An in vivo screen of mice with defects in dominant classical and lipid antigen presentation (β2M and CD1d) revealed that neither of these pathways was required for the effect of *C. accolens* on γδ T17 (Fig. S2, A and B). Further, MINCLE (CLEC4E), a receptor previously shown to be involved in the recognition of bacterial fatty acid derived from *Mycobacterium tuberculosis* (Matsunaga and Moody, 2009); CARD9, a downstream signaling mediator for several C-type lectin receptors; or MyD88, a signal transducer downstream of most Toll-like receptors, was not required to mount a response to *C. accolens* in vivo (Fig. S2, C and D).

Although we could not at this stage identify the receptor or potential alternative mode of antigen presentation involved in these responses, we assessed to which extent *C. accolens* could influence the cytokine milieu in a way that promoted γδ T cell responses. In the skin, we previously showed that *S. epidermidis* was able to promote IL-17A production from the

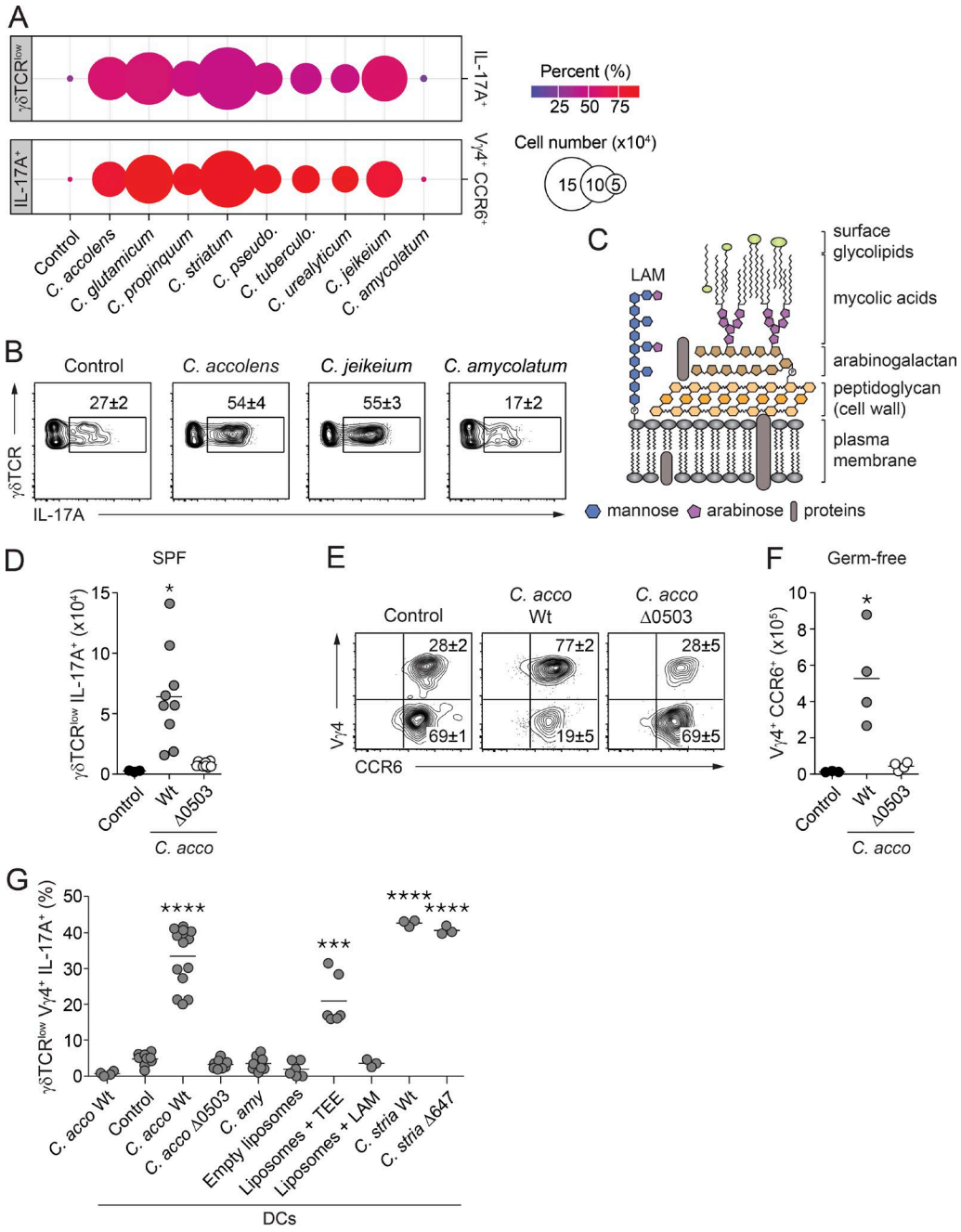

Figure 3. **The ability to induce γδ T17 cells is evolutionally conserved in the *Corybacterium* genus. (A)** Mean of absolute numbers (represented by the size of the circles) and frequencies (represented by the colors of the circles) of IL-17A–producing CD45$^+$ CD90.2$^+$ γδ TCR^{low} or γδ TCR^{low} Vγ4$^+$ CCR6$^+$ cells isolated from the skin of mice previously associated or not with various *Corynebacterium* species. **(B)** Flow cytometric plots illustrating the frequencies (mean ± SEM) of IL-17A–producing cells among skin CD45$^+$ CD90.2$^+$ γδ TCR^{low} cells from unassociated control mice or mice topically associated with *C. accolens*, *C. jeikeium*, or *C. amycolatum*. In A and B, results are representative of two independent experiments with four to six animals per group. **(C)** Schematic of the cell wall of most species of *Corynebacterium* bacteria. **(D and E)** Absolute numbers of IL-17A–producing CD45$^+$ CD90.2$^+$ γδ TCR^{low} cells (D) and flow cytometric analysis of TCR Vγ4 (Vγ4) and CCR6 expression by skin CD45$^+$ CD90.2$^+$ γδ TCR^{low} IL-17A$^+$ cells (E) isolated from SPF mice topically associated with the WT strain (*C. acco* WT) or mycolic acid synthase–deficient mutant strain (*C. acco* Δ0503) of *C. accolens*. **(F)** Absolute numbers of skin IL-17A–producing γδ TCR^{low} Vg4$^+$ CCR6$^+$ cells from GF mice topically associated with the WT strain (*C. acco* WT) or mycolic acid synthase–deficient mutant strain (*C. acco* Δ0503) of *C. accolens*. In D–F, data shown are presentative of two independent experiments with four to nine mice per group. *, $P < 0.05$ (one-way ANOVA with Holm-Šídák's multiple comparison test). **(G)** γδ TCR$^+$ Vγ4$^+$ CCR6$^+$ cells purified from the skin and/or ear-skin draining lymph nodes of *C. accolens*–associated mice were co-cultured with splenic DCs untreated (Control) or preincubated with one of the following: hk *C. accolens* WT strain (*C. acco* WT), hk mycolic acid synthase–deficient *C. accolens* mutant strain Δ0503 (*C. acco* Δ0503), hk *C. amycolatum* (*C. amy*), hk *C. striatum* WT strain

Vγ4^{neg} subset via a local increase of IL-1 (Naik et al., 2012). In contrast, based on response observed in *Il1r1*$^{-/-}$ mice, γδ T cell activation after association with *C. accolens* was IL-1 independent (Fig. 4 A). On the other hand, and consistent with the high *Il23r* gene expression in Vγ4^{+} IL-17A^{+} T cells (Riol-Blanco et al., 2010; Liang et al., 2013; Fig. 2 E), mice deficient in either IL-23R or the IL-12p40 subunit mounted a reduced response after *C. accolens* association compared with controls (Fig. 4, B and C; and data not depicted). Thus IL-23 contributes significantly to the immune impact of *C. accolens* under homeostatic conditions within the skin compartment.

To further confirm that cytokines promoted the γδ T cell response to *C. accolens*, we assessed if such a response could be reproduced in vitro. To this end, Vγ4^{+} CCR6^{+} T cells purified from the skin and regional LN of naive or *C. accolens*–associated animals were exposed to DCs loaded with hk *C. accolens* or to the filtered supernatant of these cells. DCs loaded with hk *C. accolens* or supernatants from hk *C. accolens*–loaded DCs induced a potent production of IL-17A by Vγ4^{+} γδ T cells in vitro (Fig. 4 D). Of interest and in contrast to cells isolated from preassociated mice, Vγ4^{+} γδ T cells from naive mice failed to respond when exposed to the filtered supernatant of hk *C. accolens*–loaded DCs (Fig. 4 D).

Purified DCs stimulated in vitro are likely to produce a broader range of cytokines than the relevant skin resident population, and as such we next used a more targeted approach to assess responsiveness to IL-23 and/or IL-1. Vγ4^{+} γδ T cells from *C. accolens*–associated mice were purified from the skin and submandibular LN and exposed to IL-23 or IL-1 alone. As previously shown (Holderness et al., 2013), both cytokines promoted IL-17 production by these cells when purified from naive or *C. accolens*–associated mice (Fig. 4, E and F; and Fig. S2 E). However, IL-23 was more potent than IL-1 in maximizing IL-17 production by γδ T cells (from both naive and associated mice; Fig. 4, E and F; and Fig. S2 E). This is consistent with the high level of IL-23R expression on Vγ4^{+} γδ T cells (Fig. 2 E; Cai et al., 2011; Riol-Blanco et al., 2014), a feature that may predispose them to preferentially respond to a minute increase in the IL-23 level. Of interest, Vγ4^{+} γδ T cells from *C. accolens*–associated mice had a heightened response to cytokine in vitro compared with Vγ4^{+} γδ T cells isolated from naive mice, further supporting the idea of a potential education or memory-like phenotype after association (Fig. 4, E and F; and Fig. S2 E). Such a phenomenon has been previously reported in the context of experimental psoriasis in which Vγ4^{+} γδ T cells can acquire a memory-like phenotype characterized by a heightened and more rapid response to inflammatory cytokines (Ramírez-Valle et al., 2015). Together, these results support a dominant role for IL-23 in mediating the impact of *Corynebacterium* on skin immunity.

C. accolens has a context-dependent proinflammatory effect

Although under homeostatic conditions, the *C. accolens* targeted effect on Vγ4^{+} γδ T cells is uncoupled from inflammation, this microbe may condition the tissue for subsequent inflammatory disorders. Supporting this hypothesis, in mice with defective barrier function, *C. bovis* was shown to contribute to the inflammatory process (Kobayashi et al., 2015), and in humans, the cutaneous microbiota of psoriatic lesions is characterized by an abundance of isolated *Corynebacterium* species (Gao et al., 2008; Alekseyenko et al., 2013). In a model of experimental psoriasis induced by topical application of a TLR7 agonist (imiquimod [IMQ]), part of the inflammatory processes is mediated by Vγ4^{+} γδ T cells (Gray et al., 2013; Ha et al., 2014). To evaluate if, under this setting, *C. accolens*–induced Vγ4^{+} γδ T17 cells could exacerbate skin inflammation, mice were preassociated with the bacteria 2 mo before topical treatment with IMQ. At 2 mo after association, the representation of *C. accolens* was minimal compared with other members of the skin microbiota (Fig. 1 H). Although *C. accolens* alone had no inflammatory impact on the skin, animals preassociated and subsequently treated with IMQ had significantly increased skin thickness and cellular infiltrate compared with unassociated controls (Fig. 5 A and Fig. S3, A, C, and D).

Increased inflammation was associated with higher IL-17A production from Vγ4^{+} γδ T cells in the skin of preassociated animals treated with IMQ compared with IMQ alone (Fig. 5 B) and was Vγ4^{+} subset dependent (Fig. S3 B). Thus *C. accolens*, even when present at low levels, can promote activation of Vγ4^{+} γδ T17 cells, which in turn can increase skin inflammatory responses. Increased inflammation in the context of *C. accolens* was also associated with a selective increase in inflammatory monocytes but not in neutrophils, eosinophils, or TCRβ^{+} cells (Fig. S3 D). In contrast to *C. accolens*, we found that *C. amycolatum* did not exacerbate IMQ-induced inflammation, supporting the idea that cell envelope components are required for this effect (Fig. 5 C and Fig. S3, C and D).

The outcome of *C. accolens* encounters with the skin may also depend on the physiological status of the host. Obesity has been linked to an increased prevalence of skin inflammatory disorders (Padhi and Garima, 2013). To test if host metabolic alterations could impact host responses to the commensal, we fed SPF mice with either a control or synthetic high-fat diet for 1 mo, before cutaneous association with *C. accolens*. Of note, we associated mice at an early time point after the diet change, before the development of metabolic syndrome and tissue inflammation (Zhang et al., 2015). Unassociated animals fed a high-fat diet had a modest increase in skin thickness compared with their counterparts fed a control

(*C. striatum* WT), or LAMs/lipomannans-deficient *C. striatum* (*C. stria* Δ647); liposomes containing TEEs from *C. accolens* WT strain (Liposomes + TEE) or LAMs (Liposomes + LAM); or empty liposomes. Graph illustrates the frequencies of IL-17A–producing Vγ4^{+} CCR6^{+} cells in overnight co-cultures. Graph is a compilation of the results from three to four experiments (each dot represents one culture well). ****, $P < 0.0001$ (two-tailed, unpaired Student's *t* test).

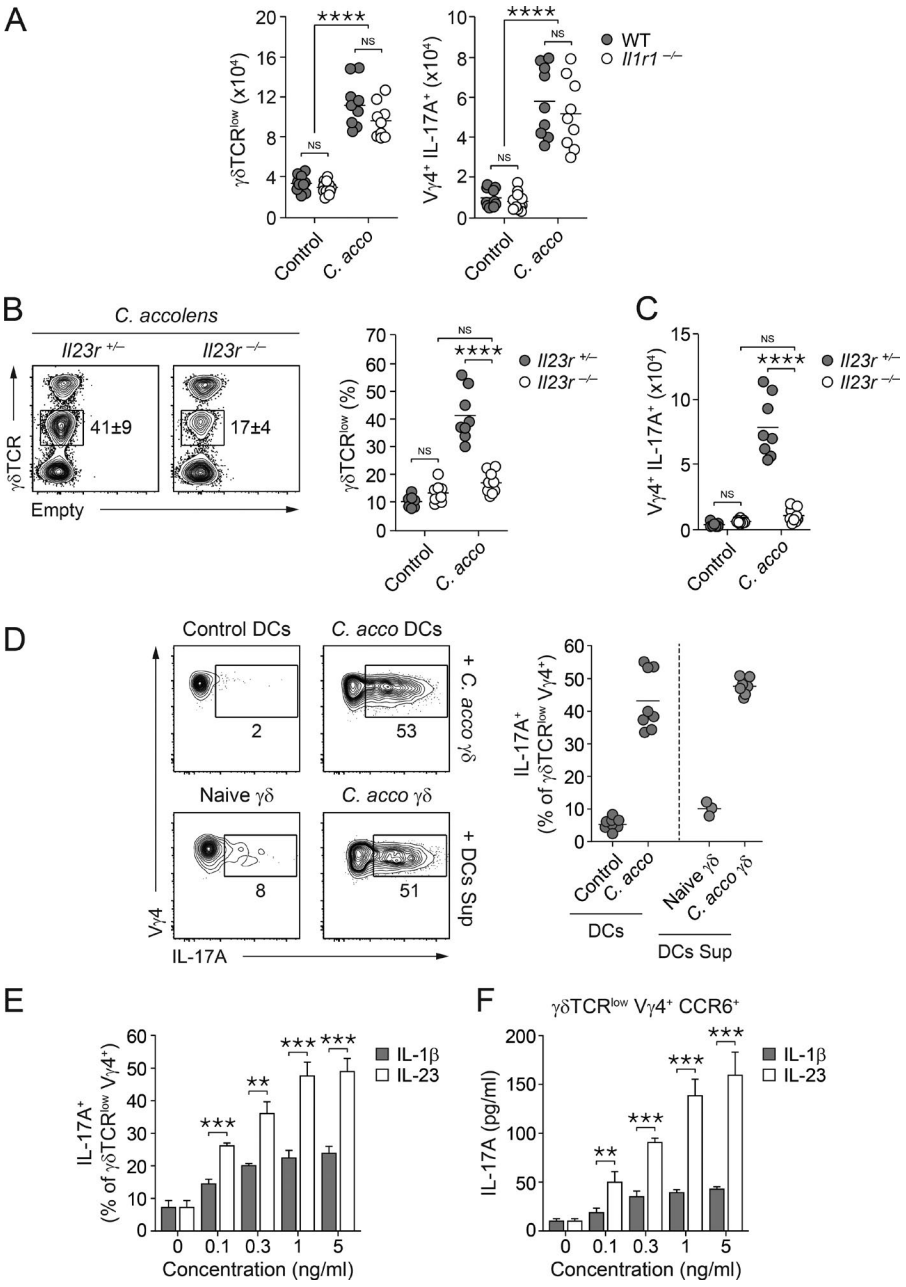

Figure 4. **IL-23 is important for γδ T17 expansion and activation in the skin after *C. accolens* topical association. (A)** Absolute numbers of total γδ TCR^{low} cells and IL-17A–producing γδ TCR^{low} Vγ4$^+$ cells in the skin of unassociated control and associated WT C57BL/6 (WT) or C57BL/6 *Il1r1*$^{-/-}$ (*Il1r1*$^{-/-}$, backcrossed to C57BL/6 for at least 10 generations) mice. **(B)** Frequencies of CD45$^+$ CD90.2$^+$ γδ TCR^{low} cells in the skin of unassociated (Control) and *C. accolens*–associated (*C. acco*) *Il23r*$^{-/-}$ and littermate control (*Il23r*$^{+/-}$) mice 2 wk after the first topical association. Flow plots illustrate cells from associated mice. **(C)** Absolute numbers of skin γδ TCR^{low} Vγ4$^+$IL-17A$^+$ cells in *Il23r*$^{-/-}$ and littermate control (*Il23r*$^{+/-}$) mice 2 wk after the *C. accolens* topical association. Control mice were left unassociated. In A–C, data shown are representative of three independent experiments with 3–11 mice per groups. ***, P < 0.001; ****, P < 0.0001; NS, not significant as calculated using two-way ANOVA with Holm-Šídák's correction for multiple hypothesis. **(D)** γδ TCR$^+$ Vγ4$^+$ CCR6$^+$ cells purified from the skin and ear-skin draining lymph nodes of naive (Naive γδ) or *C. accolens*–associated mice (*C. acco* γδ) were either co-cultured with splenic DCs preincubated with hk *C. accolens* (*C. acco* DCs) or not (Control DCs) or treated with the supernatant from DCs preincubated with hk *C. accolens* (DCs sup). Flow plots and graph illustrate the frequencies of IL-17A–producing Vγ4$^+$ CCR6$^+$ cells in overnight cultures. Flow plots are representative of three independent experiments. The graph is a compilation of the results from those three experiments (each dot represents one culture well). **(E and F)** Frequencies of IL-17A–producing Vγ4$^+$ CCR6$^+$ cells (E) and concentration of IL-17 in the supernatant (F) of overnight cultures of γδ TCR$^+$ Vγ4$^+$ CCR6$^+$ cells (purified from the skin and ear draining lymph nodes of *C. accolens*–associated mice) treated with various concentrations of recombinant mouse IL-1β or IL-23. Each bar graph represents the mean frequency or mean concentration (±SD) of triplicate cultures. Data shown are representative of two independent experiments. **, P < 0.01; ***, P < 0.001 as calculated by two-tailed, unpaired Student's *t* test.

diet (Fig. S3 E). On the other hand, and in contrast with control-diet-fed animals, mice fed a high-fat diet and associated with *C. accolens* had a significant increase in skin thickness within 2 d of association (Fig. 5 D). Interestingly, other populations of γδ T cells (Vγ4^{neg} γδ T) were also increased under these settings (Fig. 5 E); however, depleting Vγ4$^+$ cells (Fig. S3 F) abrogated this inflammatory response (Fig. 5 D). 16S rRNA gene profiling revealed that the colonization efficiency of *C. accolens* was lower in animals fed a high-fat diet compared with control-diet counterparts, supporting the idea that enhanced inflammation was not caused by aberrant *C. accolens* colonization (Fig. S3 G).

In agreement with the targeted effect of *C. accolens* in mice fed a control diet, a small number of transcripts (48 up-regulated and 31 down-regulated) modestly changed (twofold average) after association (Fig. 5 F). In contrast, application of *C. accolens* to the skin of a high-fat-fed animal was associated with a broad change in gene expression (599 up-regulated and 511 down-regulated; Fig. 5 F). Pathway analysis revealed that the majority of highly up-regulated

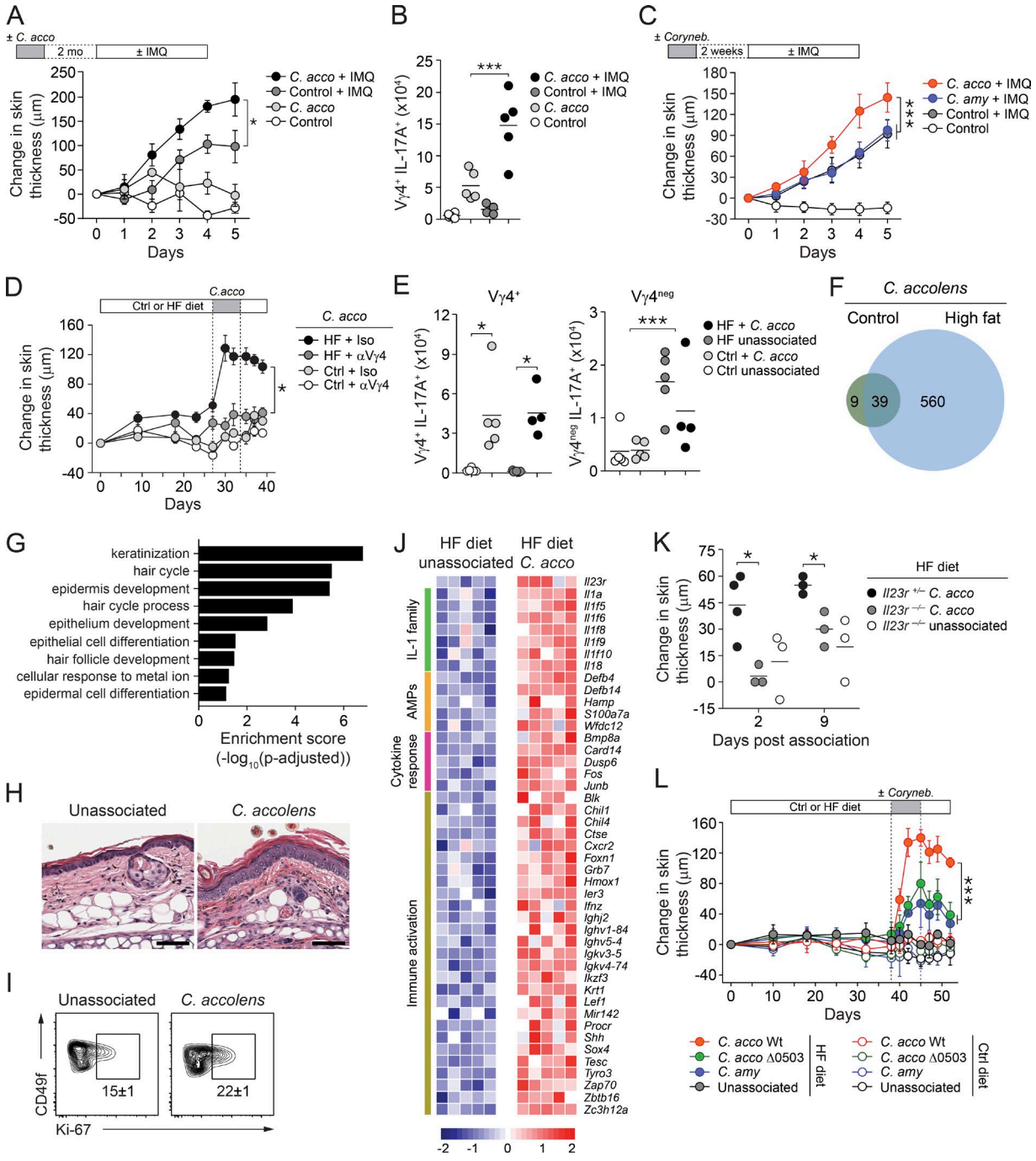

Figure 5. ***C. accolens* has a contextual proinflammatory effect. (A)** IMQ was applied daily on the ears of unassociated mice (Control) or mice topically associated with *C. accolens* (*C. acco*, every other day for 1 wk) starting 2 mo after the first topical association. The daily ear-skin thickness measurement is reported as the change in ear-skin thickness (mean ± SEM) relative to baseline at day 0 (first day of IMQ application). *, $P < 0.05$ (two-way ANOVA with Holm-Šídák's correction for multiple hypotheses). **(B)** Absolute numbers of γδ TCR^{low} Vγ4$^+$ IL-17A$^+$ cells at day 5 after the start of IMQ application in the skin of mice from A. **(C)** IMQ was applied daily on the ears of unassociated mice (Control), *C. accolens*–associated mice (*C. acco*), or *C. amycolatum*–associated mice (*C. amy*) starting 2 wk after the first topical association. The daily ear-skin thickness measurement is reported as the change in ear-skin thickness (mean ± SEM) relative to baseline at day 0 (first day of IMQ application). In A–C, data shown are representative of two to three independent experiments with five to eight mice per group. *, $P < 0.05$; ***, $P < 0.005$ as calculated using two-way ANOVA with Holm-Sidak's correction for multiple hypothesis. (**D–J**) 3-wk-old mice were fed either a high-fat (HF) or a control (Ctrl) diet for 1 mo before topical association with *C. accolens*. Mice were treated with anti-Vγ4 (αVγ4) or isotype control antibodies (Iso) starting on the first day of *C. accolens* topical association. (D) The ear-skin thickness measurement is reported as the change in ear-skin thickness (mean ± SEM) relative to baseline at day 0 (first day given the high-fat or control diet). (E) Absolute numbers of

gene ontology (GO) pathways were linked to keratinocyte/hair follicle responses (Fig. 5 G). Histological assessment revealed hyperkeratinization in *C. accolens*/high-fat animals compared with unassociated controls and, as assessed by flow cytometry, enhanced keratinocyte proliferation (Fig. 5, H and I). Expression of numerous immune-related genes was also up-regulated, including those known to contribute to skin inflammation, such as genes encoding for several members of the IL-1 family as well as IL-23R (Fig. 5 J). Nonetheless, no changes in cellular infiltrate (neutrophils, eosinophils, and monocytes) were observed in the context of *C. accolens*/high-fat diet compared with high-fat diet alone, supporting the idea that changes in skin physiology result dominantly from a targeted impact on keratinocytes (Fig. S3 H). Thus, in the context of a high-fat diet, the addition of an innocuous skin microbe can be sufficient to trigger inflammation. The rapid inflammatory impact of *C. accolens* on the skin of high-fat-diet–fed mice was significantly reduced in IL-23R–deficient mice, further implicating this cytokine in mediating the effect of *C. accolens* in both steady state and inflammation (Fig. 5 K).

We next tested if the expression of mycolic acid could mediate the pathogenic impact of *C. accolens*. To this end, high-fat-diet–fed mice were associated with WT or Δ0503 *C. accolens* or *C. amycolatum*. To normalize colonization by the Δ0503 mutant, mice were associated daily starting 4 wk after introduction of the high-fat diet. As previously shown, *C. accolens* alone induced skin inflammation as early as 2 d after association. In contrast, the impact of *C. accolens* Δ0503 or *C. amycolatum* was significantly reduced compared with high-fat-diet–fed mice associated with control bacteria (Fig. 5 L). Thus, mycolic acid expression is associated with the pathogenic effect of *Corynebacterium*. These results also reveal that host metabolic status can have a profound impact on the sensing and interpretation of microbial signals by the host's immune system and may predispose to inflammatory responses to an otherwise commensalistic or mutualistic symbiont.

Despite the growing understanding that microbes are critical to the promotion of skin immunity, the microbial determinants responsible for mediating these interactions remain undefined. Our data demonstrate that *Corynebacterium* activates the skin immune system and that this property depends on the expression of mycolic acid, a highly conserved surface molecule that distinguishes *Corynebacteria* from other gram-positive skin microbes. Together, our results also reveal that host metabolic status can have a profound impact on the sensing and interpretation of microbial signals by the host's immune system and may profoundly impact the outcome of the host–immune system encounter. Our data show that skin microbes can, in a predisposed skin state, be sufficient to trigger inflammation. Moreover, they reveal that a change in diet alone can be sufficient to transform a mutualistic member of the skin microbiota into an inflammatory trigger. In contrast to the gut, the skin is characterized by a scarcity of nutrients available to fuel the microbiota (Scharschmidt and Fischbach, 2013). In these arid conditions, subtle alterations in nutrient availability can potentially have a dramatic impact on the impact of the skin microbiota. Obesity has been linked to the increased severity and prevalence of many skin inflammatory disorders (Padhi and Garima, 2013). Based on our present findings, it is intriguing to consider that these effects may be, in part, mediated by altered responses to canonical microbial components. Further, based on the prevalence of *Corynebacteria* on mammalian skin and the ability of this genus to selectively engage IL-23–dependent responses, our work may have identified a dominant mediator of skin immunity and inflammation. Clinical observations have implicated IL-23 signaling in inflammatory diseases, and this cytokine is now considered a major therapeutic target in immune-based pathologies such as psoriasis (Puig, 2017). Furthermore, in the context of inflammation-related cancer, IL-23 is thought to

skin IL-17A-producing γδ TCR^{low} Vγ4^{+} and γδ TCR^{low} Vγ4^{neg} cells in unassociated or associated mice (day 14 after the first topical association) fed high-fat or control diet. In D and E, data shown are representative of two to three independent experiments with three to five mice per group. *, $P < 0.05$; ***, $P < 0.005$ as calculated using two-way ANOVA with Holm-Šídák's correction for multiple hypothesis. (F) Venn diagram analysis comparing all statistically up-regulated genes in the skin between mice given control and high-fat diets after *C. accolens* association. (G) Pathway analysis was performed using Enrichr based on all genes up-regulated in the skin of mice given the high-fat diet after *C. accolens* association. Top 9 GO pathways are shown based on enrichment score (−log10 [adjusted p-value]). (H) Representative histopathological comparison of the ear pinnae of unassociated and *C. accolens*–associated mice given a high-fat diet at day 14 after the first topical association. Bars, 50 µm. (I) Frequencies (mean ± SEM) of Ki67^{+} keratinocytes (CD45^{neg} CD31^{+} CD34^{+} Sca-1^{+}) in the skin of unassociated and *C. accolens*–associated mice given a high-fat diet (day 14 after association). In H–I, data shown are representative of two independent experiments. (J) Heat map of immunology-related genes statistically differentially expressed in the skin (ear pinnae) of unassociated and *C. accolens*–associated mice given a high-fat diet. Each row of the heat map represents gene expression from the two ears (pooled) of one mouse ($n = 5$ per group). **(K)** 3-wk-old *Il23r*$^{-/-}$ and littermate control (*Il23r*$^{+/-}$) mice were fed a high-fat (HF) diet for 1 mo prior being topically associated with *C. accolens* or not. The ear-skin thickness measurement is reported as the change in ear-skin thickness (mean ± SEM) relative to baseline at day 0 (first day given the high-fat diet). Data shown are representative of two independent experiments with three to four mice per group. *, $P < 0.05$ as calculated using two-tailed, unpaired Student's *t* test. **(L)** 3-wk-old mice were fed either a high-fat (HF) or a control (Ctrl) diet for 1 mo before topical association with the WT strain (*C. acco* Wt) or corynomycolic acid synthase–deficient mutant strain (*C. acco* Δ0503) of *C. accolens* or with *C. amycolatum* (*C. amy*). The ear-skin thickness measurement is reported as the change in ear-skin thickness (mean ± SEM) relative to baseline at day 0 (first day given the high-fat or control diet). Data shown are representative of two independent experiments with five mice per group. ***, $P < 0.005$ as calculated using two-way ANOVA with Holm-Šídák's correction for multiple hypotheses.

contribute to tumorigenesis and progression to metastatic disease (Langowski et al., 2006; Wang and Karin, 2015). The ability of *Corynebacteria* to promote IL-23 signaling, an effect that can potentially target numerous immune populations within the skin environment, including classical T cells, could be highly relevant to the etiology of a variety of skin disorders in humans.

Together, our present results support the idea that a dominant genus of the skin microbiota has a profound impact on both skin immunity and inflammation and that canonical cell envelope components from these microbes may represent a dominant skin microbiota signal. Further, our results support the idea that conserved microbial determinants from an innocuous colonist can have a highly context-specific effect on the skin immune system and that in the skin a simple diet alteration can have a dramatic effect on the ability of the host to integrate microbe-derived signals. Although understanding the mechanism of interaction between the immune system and the microbiota remains in its infancy, this line of investigation is required not only to understand the impact of defined microbial communities on skin physiology but also as a means to uncover novel classes of immunological adjuvants.

MATERIALS AND METHODS

Subjects and ethics

Human skin swabs were obtained from anonymous healthy volunteers. All volunteers gave written informed consent, and collection of skin swabs was conducted according to the principles of the declaration of Helsinki after approval by the Institutional Review Board of National Institute of Allergy and Infectious Diseases (NIAID), National Institutes of Health (NIH).

Mice

C57BL/6 SPF mice were purchased from Taconic Farms. GF C57BL/6 mice were bred and maintained in the NIAID Microbiome Program gnotobiotic animal facility. B6.SJL-Cd45a(Ly5a)/Nai (B6.SJL), C57BL/6-[KO] IL17A (*Il17a*$^{-/-}$), C57BL/6NTac-[KO]β2m (*B2m*$^{-/-}$), and C57BL/6-[KO]IL1r1 (*Il1r1*$^{-/-}$) mice were obtained through the NIAID-Taconic exchange program. B6.129S6-Del(3Cd1d2-Cd1d1)1Sbp/J (*Cd1d*$^{-/-}$) mice and their C57BL/6J WT controls were purchased from the Jackson Laboratory. *Il22*$^{-/-}$ mice were generated by Pfizer Inc. *Il23r*$^{-/-}$ mice (Awasthi et al., 2009) were obtained by breeding *Il23r*$^{eGFP+/-}$ reporter mice (a gift from M. Oukka, Seattle Children's Research Institute, Seattle, WA) to generate *Il23r*$^{eGFP+/eGFP+}$ (*Il23r*$^{-/-}$) and *Il23r*$^{eGFP+/-}$ (littermate control) mice. B6.129P2-*Myd88*^{tmAki} (*Myd88*$^{-/-}$), C57BL/6 *Clec4e*$^{-/-}$ (Yamasaki et al., 2009; *Mincle*$^{-/-}$, originally generated by S. Yamasaki, Kyushu University, Fukuoka, Japan) and C57BL/6 *Card9*$^{-/-}$ (Hsu et al., 2007) mice were gifts from G. Trinchieri (National Cancer Institute/NIH, Bethesda, MD), A. Sher (NIAID/NIH, Bethesda, MD), and M. Lionakis (NIAID/NIH, Bethesda, MD), respectively, and backcrossed to C57BL/6 for at least 10 generations. For experiments with knockout mice, littermate controls were used as WT controls, and/or WT (littermate or C57BL/6) and knockout mice were cohoused at 3–4 wk of age for 2–3 wk in the same cage, and then separated before the start of experimental manipulations. All mice were bred and maintained under pathogen-free conditions at an American Association for the Accreditation of Laboratory Animal Care–accredited animal facility at the NIAID and housed in accordance with the procedures outlined in the Guide for the Care and Use of Laboratory Animals. All experiments were performed at the NIAID under an animal study proposal approved by the NIAID Animal Care and Use Committee. Sex- and age-matched mice between 6 and 12 wk of age were used for each experiment. When possible, preliminary experiments were performed to determine requirements for samples size, taking in account resources available and ethical, reductionist animal use. In general, each mouse of the different experimental groups is reported. Exclusion criteria, such as inadequate staining or low cell yield due to technical problems, were predetermined. Animals were assigned randomly to experimental groups.

Topical association

Bacillus lincheniformis and *Escherichia coli* (17KO) were isolated from the skin draining lymph nodes of *Il17a*$^{-/-}$ mice. *Candida albicans*, *E. coli* (22KO), and *Enterococcus faecalis* were isolated from the skin of the ear pinnae of *Il22*$^{-/-}$ mice. *S. epidermidis* strain NIHLM087 (Conlan et al., 2012) and *Micrococcus luteus* strain HV1032 were isolated from the skin of healthy human volunteers. All those bacteria were cultured for 18 h in tryptic soy broth at 37°C. *C. accolens* strain ATCC 49725, *C. amycolatum* strain SK46, *C. glutamicum* strain DSM 20300, *C. jeikeium* strain DSM 7171, *C. propinquum* strain DSM 44285, *C. pseudodiphtheriticum* strain DSM 44287, *C. striatum* strain DSM 20668, *C. tuberculostearicum* strain ATCC 35692, and *C. urealyticum* strain ATCC 43042 were cultured for 18 h in a brain–heart infusion broth supplemented with 1% Tween 80 (Sigma-Aldrich) at 37°C. Bacteria were enumerated before topical application by assessing CFUs using traditional bacteriology techniques and by measuring OD at 600 nm with the use of a spectrophotometer.

For topical association of bacteria, each mouse was associated with bacteria by applying bacterial suspension (5 ml, ∼10^9 CFU/ml for most experiments, or 10^8 or 10^7 CFU/ml for Fig. S1, H and I, as indicated) across the entire skin surface (∼36 cm^2) using a sterile cotton swab. Application of bacterial suspension was repeated every other day for a total of four times (or for Fig. S1, H and I, performed only once as indicated). In experiments involving the topical application of various bacterial species or strains, 18-h cultures were normalized using OD_{600} to achieve similar bacterial density (∼10^9 CFU/ml).

IMQ model of psoriasis-like dermatitis

The induction of psoriasis-like inflammation on ear skin was done as previously described (Gray et al., 2013). Mice were treated daily for up to 5 d with 5 mg 5% IMQ cream (Aldera cream;Valeant Pharmaceuticals) topically applied on each ear. Ear-skin thickness was measured using a digital caliper (Mitutoyo). For each mouse, a daily ear-skin-thickness value was calculated by averaging the thickness of both ears.The change in ear-skin thickness over time was reported as the difference related to the first day of IMQ application.

Diet studies

The high-fat diet (TD.06414; 60% of total calories from fat) and the corresponding control diet (TD.150064; 10% of total calories from fat) were purchased from Envigo Teklad Diets. Mice were placed under those diet regimens at weaning (3 wk old) for 4 wk before topical association with bacteria. Ear thickness was measured with a digital caliper (Mitutoyo). For each mouse, the ear-skin thickness value at a defined time point was calculated by averaging the thickness of both ears measured on this time point. The change in ear-skin thickness over time was reported as the difference related to the first day the mice were first given specific diets.

In vivo antibody administration

Mice were treated i.p. with anti–TCR Vγ4 antibody (clone UC3-10A6; BioXCell) or Armenian Hamster IgG isotype control antibody (BioXCell). The treatment schedule was as follows: 0.5 mg of either antibody was injected 2 d before topical association with *C. accolens*; each mouse then received 0.5 mg of either antibody every 3 d starting on the day of the first topical association until analysis.

Tissue processing

Cells from the ear pinnae were isolated as previously described (Naik et al., 2012). Single-cell suspensions from the ear draining lymph nodes were prepared by passing tissue through a 70-µm cell strainer after digestion with 0.1 mg/ml Liberase TL purified enzyme blend (Roche) and 0.5 mg/ml DNase I (Sigma-Aldrich) for 30 min at 37°C.

In vitro restimulation

For detection of basal cytokine potential, single-cell suspensions from various tissues were cultured directly ex vivo in a 96-well U-bottom plate in complete medium (RPMI 1640 supplemented with 10% FBS, 2 mM L-glutamine, 1 mM sodium pyruvate and nonessential amino acids, 20 mM Hepes, 100 U/ml penicillin, 100 µg/ml streptomycin, and 50 mM β-mercaptoethanol) and stimulated with 50 ng/ml PMA (Sigma-Aldrich) and 5 µg/ml ionomycin (Sigma-Aldrich) in the presence of BFA (GolgiPlug; BD Biosciences) for 2.5 h at 37°C in 5% CO_2. After stimulation, cells were assessed for intracellular cytokine production as described in the next section.

Phenotypic analysis

Mouse single-cell suspensions were incubated with fluorochrome-conjugated antibodies against surface markers CCR6 (clone 29-2L17), CD4 (RM4-5), CD8β (eBioH35-17.2), CD11b (M1/70), CD11c (N418), CD19 (MB19-1), CD31 (MEC13.3), CD34 (RAM34), CD40 (IC10), CD45 (30-F11), CD45.2 (104), CD45R (RA3-6B2), CD49b (DX5), CD49f (eBioGoH3), CD64 (X54-5/7.1), CD90.2 (53–2.1), Ly6C (AL-21), Ly6G (1A8), MHC II (M5/114.15.2), NK1.1 (PK136), Sca-1 (D7), Siglec F (E50-2440), TCRβ (H57-597), TCR Vγ4 (UC3-10A6), and/or γδ TCR (eBioGL3) in HBSS for 20 min at 4°C and then washed. For CCR6 staining, cell suspensions were first incubated with antibody against CCR6 (29-2L17) for 45 min at room temperature before incubation with other fluorochrome-conjugated antibodies against surface markers for 20 min at 4°C. LIVE/DEAD Fixable Blue Dead Cell Stain kit (Invitrogen Life Technologies) was used to exclude dead cells. Cells were then fixed for 30 min at 4°C using the fixation/permeabilization buffer supplied with the BD Cytofix/Cytoperm kit (BD Biosciences) and washed twice with permeabilization buffer. For intracellular staining, cells were then stained with fluorochrome-conjugated antibody against IL-17A (eBio17B7 or TC11-18H10.1) and/or Ki-67 (SolA15) in permeabilization buffer supplied with the BD Cytofix/Cytoperm kit (BD Biosciences) for 1 h at 4°C. Each staining was performed in the presence of purified anti–mouse CD16/32 (93), 0.2 mg/ml purified rat IgG, and 1 mg/ml normal mouse serum (Jackson Immunoresearch). All antibodies were purchased from BD Biosciences, Biolegend, eBioscience, or R&D Systems. Cell acquisition was performed on an LSR Fortessa flow cytometer using FACSDiVa software (BD Biosciences), and data were analyzed using FlowJo software (TreeStar).

Analysis of skin microbiota

DNA extraction from skin and sequencing. Mouse ear pinnae skin samples were sterilely obtained and processed using a protocol adapted from (Grice et al., 2010). For 16S rRNA amplicon Illumina MiSeq sequencing, the DNA from each sample was amplified using Accuprime High Fidelity Taq polymerase (Invitrogen Life Technologies) with universal primers flanking variable regions V1 (primer 27F; 5′-AGAGTTTGATCCTGGCTCAG-3′) and V3 (primer 534R; 5′-ATTACCGCGGCTGCTGG-3′). For each sample, the universal primers were tagged with unique sequences (“barcodes”) to allow for multiplexing/demultiplexing. PCR products were then purified using the Agencourt AmPure XP kit (Beckman Counter Genomics) and quantitated using the QuantIT dsDNA High-Sensitivity Assay kit (Invitrogen Life Technologies). Approximately equivalent amounts of each PCR product were then pooled and purified using Agencourt AMPure magnetic beads before sequencing on an MiSeq instrument (Illumina). Sequencing data were analyzed as previously described (Naik et al., 2012). Data deposition is with the Sequence Read Archive and all sequences can be accessed under BioProject ID no. PRJNA389472 (www.ncbi

.nlm.nih.gov/bioproject/389472) and no. PRJNA384162 (www.ncbi.nlm.nih.gov/bioproject/384162).

Bacteria quantitation. The ear pinnae of topically associated or unassociated control mice were swabbed with a sterile cotton swab previously soaked in brain–heart infusion broth supplemented with 1% Tween 80. Swabs were streaked on Columbia blood agar plates. Plates were then placed at 37°C under aerobic conditions for 18 h. CFUs on each plate were enumerated, and the number of CFUs was reported per square centimeter of skin.

Gene expression analysis

NanoString. $V\gamma4^+$ $CCR6^+$ γδ T cells ($CD45^+CD90.2^+$ γδ TCR^{low} TCR $V\gamma4^+$ $CCR6^+$, >95% purity) were isolated from the skin of unassociated mice or mice associated with *S. epidermidis* or *C. accolens* strain ATCC 49725 (day 14 after association) by cell sorting using a FACSAria cell sorter (BD Biosciences). The nCounter analysis system (NanoString Technologies) was used to screen for the expression of signature genes associated with lymphocyte activation. In brief, RNA from each sample was obtained by lysing the sorted cells (10^3 cells/µl) in RLT buffer (Qiagen) and then hybridized with the customized Reporter CodeSet and Capture ProbeSet of a custom NanoString chip (132 genes; Table S1), according to the manufacturer's instructions. mRNA molecules were counted on a NanoString nCounter. Data analysis was performed according to NanoString Technologies recommendations. mRNA counts were processed to account for hybridization efficiency, background noise, and sample content using the R package NanoStringNorm with arguments: CodeCount = "geo.mean," Background = "mean.2sd," and SampleContent = "housekeeping.geo.mean." Each sample profile was normalized to geometric mean of three housekeeping genes (*Eef1g*, *Gusb*, and *Oaz1*). After normalization, genes with mean counts less than two SDs above the mean count of the highest negative control (count > 4.34092) were disregarded, and differential expression of remaining genes was determined using a nonparametric Welch *t* test with correction for multiple testing using the Benjamini-Hochberg false discovery rate controlling procedure in the multtest package in R. By using those genes with a false discovery rate <0.05, a heatmap was rendered using the R package pheatmap.

Microarray. For gene expression analysis by microarray of total tissue homogenate, ear pinnae were isolated from unassociated control mice or mice previously associated with *C. accolens* strain ATCC 49725 (day 14 after association) and stored in RNAlater until RNA extraction. In brief, tissues were lyzed in TRIzol reagent (Invitrogen/Life Technologies) using bead disruption, and total RNA was extracted using phenol/chloroform extraction followed by the miRNeasy kit (Qiagen) according to the manufacturer's instructions. Total RNA was then used for GeneChip analysis using the Mouse Gene 2.0 ST Array (Affymetrix). Terminal-labeled cDNA synthesis, hybridization to genome-wide Mouse Gene 2.0 ST GeneChips, and scanning of the arrays were performed according to the manufacturer's instructions (Affymetrix). The microarray data discussed in this publication have been deposited in the Gene Expression Omnibus (GEO) database under accession no. GSE96932. Pathway analysis was performed using Enrichr (http://amp.pharm.mssm.edu/Enrichr/; Kuleshov et al., 2016) based on all genes up-regulated between samples from unassociated and associated mice given the high-fat-diet treatment. Redundant gene lists obtained from the GO term database on the Enrichr site were collapsed. The top nine GO pathways are shown based on enrichment score (−log10 [adjusted P value]).

Construction of *Corynebacterium* mutants

C. accolens Δ0503, a mutant devoid of mycolic acids, was constructed in the *C. accolens* background ATCC 49725 by replacing the gene encoding mycolic acid condensase (locus tag: HMPREF0276_0503) with a 21-bp in-frame scar. *C. striatum* Δ647, a mutant devoid of LAMs and lipomannans, was similarly constructed in the *C. striatum* background DSM 20668 by replacing the gene encoding the proximal mannan chain elongase (locus tag: HMPREF0276_0647) with a 21-bp in-frame scar. To make each deletion construct, ∼1.2- to 1.5-kb flanking regions up- and downstream of each gene were amplified with the following primer pairs, with the scar sequence underlined: JC_0503UP_F (5′-CAATTGCGGATCCGCCTTCTTGCAGTACACCTCCGGC-3′)/JC_0503UP_R (5′-CCCATCCACTAAACTTAAACACATAAACCGTCTTTCCTAGTGG-3′) and JC_0503DOWN_F (5′-TGTTTAAGTTTAGTGGATGGGTGAGAAGCTCGCTGACCTG-3′)/JC_0503DOWN_R (5′-CGAATTCTGCAGCTAGTTAATATCGCCGCTCAAGTTCTTCGACCC-3′); and JC_0647UP_F (5′-CAAGACAATTGCGGATCCAGCCATGTTCTCCGTGTTGATG-3′)/JC_0647UP_R (5′-CCCATCCACTAAACTTAAACACAGTGAGACGCTGTTTCATAAAG-3′) and JC_0647DOWN_F (5′-TGTTTAAGTTTAGTGGATGGGAGTGTCCTAAACTAGTCCTTCGTG-3′)/JC0647UP_R (5′-AAGCTTCGAATTCTGCAGCTCGACAACACCCATGAGAATG-3′).

The flanking fragments were then assembled by circular polymerase extension cloning (Quan and Tian, 2011) into pJSC232 (Converse and Cox, 2005), which was first amplified with primer pair JC_pJSC_F (5′-GCGGCGATATTAACTAGCTGCAGAATTCGAAGCTTATCG-3′)/JC_pJSC_R (5′-GGTGTACTGCAAGAAGGCGGATCCGCAATTGTCTTGGATCGG-3′) to generate ends compatible with the inserts. The circular polymerase extension cloning reaction of each resulting deletion construct was introduced into *E. coli* Top10 by electroporation, and both deletion constructs were verified by colony PCR and sequencing.

Competent *C. accolens* and *C. striatum* cells were generated as previously described for *C. glutamicum* (Eggeling and Bott, 2005) with the following adaptations. Cells were cultivated in brain–heart infusion sorbitol medium supple-

mented with 1% (wt/vol) of Tween 80 (BHIST), and cultures were incubated at 37°C. 2 µg of each deletion construct was introduced into a 150-µl aliquot of fresh, competent *C. accolens* or *C. striatum* by electroporation in a 0.2-cm cuvette (at 25 µF, 200 Ω, and 2.5 kV on a MicroPulser; Biorad) and immediately heat-shocked for 6 min at 46°C. The cells were allowed to recover for 90–120 min with shaking at 37°C before plating on BHIST plus 15 µg/ml kanamycin (Km). The plates were then incubated for 3–4 d at 37°C to obtain single crossover integrants, verified by colony PCR. Double-crossovers were obtained by plating single crossovers on brain–heart infusion plus 1% (wt/vol) Tween 80, supplemented with 20% sucrose to allow for counterselection of the sacB marker on the pJSC232 backbone. Deletion of the native gene was verified by colony PCR. We could not detect any extractable corynomycolic acids in *C. accolens* Δ0503 after whole-cell methanolysis (Minnikin et al., 1980). The colony morphology and growth defect are consistent with the equivalent mutant in *C. glutamicum* (Gande et al., 2004). In *C. striatum* Δ647, lipoglycan extraction and analysis by SDS-PAGE gel showed no bands corresponding to LAMs or lipomannans, similar to the equivalent mutant in *C. glutamicum* (Mishra et al., 2008).

Preparation of liposomes

TEEs were prepared from the cell pellets of 48-h cultures of *C. accolens* strain ATCC 49725. Cell pellets were first washed in distilled water and then subjected to extraction for 16 h with chloroform/methanol (1:2 vol/vol) at room temperature, followed by reextraction with chloroform/methanol (1:1 vol/vol) and finally with chloroform/methanol (2:1 vol/vol) for 16 h each (Bou Raad et al., 2010). The three organic phases resulting from the extraction procedures were pooled, concentrated by means of rotary evaporation, and then partitioned between aqueous and organic phases using a mixture of chloroform/water (1:1 vol/vol). The organic phase was retained and evaporated to dryness yielding the TEEs from *C. accolens*. Liposomes were prepared as previously described (Korf et al., 2005). 250 µg TEE or LAM from *Mycobacterium smegmatis* (Invivogen) was mixed with 45 µl L-α-phosphatidylcholine at 100 mg/ml in chloroform (Sigma-Aldrich). Empty liposomes were used as a negative control. Liposomes were dried down and dissolved with sonication in 1 ml PBS before use in mononuclear phagocytes–γδ T cell co-culture assays.

Dendritic cell–γδ T cell co-culture assay

Vγ4$^+$ CCR6$^+$ γδ T cells (CD45$^+$CD90.2$^+$ γδ TCR^{low}TCR Vγ4$^+$ CCR6$^+$, >95% purity) were sorted by flow cytometry from the ear-skin tissue and ear draining lymph nodes of C57BL/6 mice 2 wk after topical association with *C. accolens* strain ATCC 49725 using a FACSAria cell sorter. For splenic DC purification, single-cell suspensions from the spleen of congenic WT mice were magnetically enriched for CD11c$^+$ cells by positive selection using CD11c MicroBeads and MACS separation columns (Miltenyi Biotec). Purified DCs and Vγ4$^+$ CCR6$^+$ γδ T cells were co-cultured at a 15:1 ratio (10^4 Vγ4$^+$ CCR6$^+$ γδ T cells) in a 96-well U-bottom plate in complete medium for 16–18 h at 37°C in 5% CO_2. BFA (GolgiPlug) was added for the final 4 h of culture. DCs were previously incubated for 2 h with or without hk *C. accolens* strain ATCC 49725 (WT), hk corynomycolic acid synthase–deficient *C. accolens* strain Δ0503, hk *C. amycolatum*, hk *C. striatum* strain DSM 20668 (WT), or hk *C. striatum* mutant strain Δ647 (bacteria/DCs ratio, 500:1) and washed before co-culture with Vγ4$^+$ CCR6$^+$ γδ T cells. For some experiments, DCs were preincubated with 100 µl of one of the following liposome suspensions prepared as described in the previous section—empty liposomes or liposomes containing one of the following: *C. accolens* TEE, or LAM from *M. smegmatis*. In other experiments, Vγ4$^+$ CCR6$^+$ γδ T cells (10^4) were cultured in a 96-well U-bottom plate for 16–18 h at 37°C in 5% CO_2 in presence of the filtered culture supernatant (dilution 1:3 in complete medium) of DCs incubated for 4 h with hk *C. accolens* strain ATCC 49725. IL-17A production by Vγ4$^+$ CCR6$^+$ γδ T cells after co-culture was assessed by flow cytometry after intracellular cytokine staining using the following antibodies: α-CD45.1 (clone A20), α-CD45.2, α-CD90.2, α-TCRβ, α-TCR Vγ4, α-γδ TCR, and α-IL-17A.

Cytokine measurement

FACS-purified CD45$^+$ CD90.2$^+$ γδ TCR^{low} TCR Vγ4$^+$ CCR6$^+$ T cells from the skin of naive unassociated or *C. accolens*–associated mice were cultured overnight at 37°C in 5% CO_2 in 200 µl complete culture medium in a 96-well U-bottom plate in the presence or absence of various concentrations of recombinant IL-1β or IL-23 (Peprotech). Supernatants were collected, and levels of IL-17 were assessed using a bead-based cytokine detection assay (FlowCytomix, eBioscience).

Histology

Mice were euthanized 14 d after topical application of *C. accolens* strain ATCC 49725. Unassociated mice were used as controls. The ears from each mouse were removed and fixed in PBS containing 10% formalin. Paraffin-embedded sections were cut at 0.5 mm, stained with hematoxylin and eosin, and examined histologically.

Statistics

Data are presented as mean ± SEM or mean ± SD. Group sizes were determined based on the results of preliminary experiments. Mice were assigned at random to groups. Mouse studies were not performed in a blinded fashion. Generally, each mouse of the different experimental groups is reported. Statistical significance was determined using one of the following statistical tests: one-way or two-way ANOVA or two-tailed unpaired Student's *t* test under the untested assumption of normality. Two-way ANOVA was used to determine if a specific immune phenotype was affected by two factors, in an independent manner or because of an interaction of factors studied. We

used a Holm-Šídák test for correction for multiple hypotheses. Within each group there was an estimate of variation, and the variance between groups was similar. All statistical analysis was calculated using Prism software (GraphPad). Differences were considered to be statistically significant when $P < 0.05$.

Online supplemental material

Fig. S1 shows the impact of diverse skin commensal microbes on various populations of immune cells in the skin, the absence of inflammation after cutaneous association with *C. accolens*, as well as the number of CFUs present on the ear pinnae and the impact of *C. accolens* after topical application with various doses of bacteria. Fig. S2 shows the absolute numbers of $V\gamma4^+$ $IL\text{-}17A^+$ cells in the skin of WT, *B2m*$^{-/-}$, *Cd1d*$^{-/-}$, *Clec4e*$^{-/-}$, *Card9*$^{-/-}$, and *Myd88*$^{-/-}$ mice after association with *C. accolens*, as well as IL-17 secretion by skin $\gamma\delta TCR^+V\gamma4^+$ $CCR6^+$ cells from naive mice after treatment with IL-1 or IL-23. Fig. S3 shows the change in skin thickness and absolute numbers of $V\gamma4^+$ $IL\text{-}17A^+$ cells, neutrophils, inflammatory monocytes, and $TCR\beta^+$ cells in the skin after IMQ topical application in mice previously associated 2 wk earlier with *C. accolens* or *C. amycolatum* compared with unassociated control mice. In addition, Fig. S3 shows the change in skin thickness in unassociated mice receiving a control or high-fat diet, as well as absolute numbers of neutrophils, eosinophils, and inflammatory monocytes in unassociated and *C. accolens*–associated mice given a high-fat or control diet regimen. Table S1 shows the gene list of the custom NanoString CodeSet used to analyze activation-associated lymphocyte gene expression.

ACKNOWLEDGMENTS

We thank the National Institute of Allergy and Infectious Diseases (NIAID) animal facility staff, in particular, D. Trageser-Cesler and C. Acevedo (NIAID Microbiome Program Gnotobiotic Animal Facility); K. Beacht and J. LeGrand for technical assistance; J. Davis (NIAID Microbiome Program Sequencing); Dr. A.G. Elkahloun (National Human Genome Research Institute Microarray Core); Dr. G. Trinchieri (*Myd88*$^{-/-}$ mice); Dr. A. Sher (*Clec4e*$^{-/-}$ mice); and Dr. M. Lionakis (*Card9*$^{-/-}$ mice). We also thank the Belkaid laboratory for critical reading of the manuscript.

This work was supported by the Division of Intramural Research of the NIAID, a Howard Hughes Medical Institute–Simons Foundation Faculty Scholar Award (to M.A. Fischbach), a Burroughs Wellcome Fund Investigators in the Pathogenesis of Infectious Disease Award (to M.A. Fischbach), and National Institutes of Health grants R01 AI101018, R01 DK110174, and DP1 DK113598 (to M.A. Fischbach). V.K. Ridaura and M.G. Constantinides are Cancer Research Institute Irvington Fellows supported by the Cancer Research Institute. S. Tamoutounour is supported by a European Molecular Biology Organization Long-Term Fellowship.

The authors declare no competing financial interests.

Author contributions: V.K. Ridaura, N. Bouladoux, Y. Belkaid, and M.A. Fischbach designed the studies. V.K. Ridaura, N. Bouladoux, J. Claesen, and Y. Erin Chen performed experiments and analyzed the data. M.G. Constantinides and E.D. Merrill assisted with in vitro co-culture studies and in vivo treatment with IMQ, respectively, and provided valuable intellectual input. S. Tamoutounour performed analysis of keratinocytes and dendritic cell/monocyte/macrophage populations. A.L. Byrd performed microarray data analysis. V.K. Ridaura, N. Bouladoux, and Y. Belkaid wrote the manuscript.

Submitted: 14 June 2017
Revised: 3 November 2017
Accepted: 21 December 2017

REFERENCES

Alekseyenko, A.V., G.I. Perez-Perez, A. De Souza, B. Strober, Z. Gao, M. Bihan, K. Li, B.A. Methé, and M.J. Blaser. 2013. Community differentiation of the cutaneous microbiota in psoriasis. *Microbiome.* 1:31. https://doi.org/10.1186/2049-2618-1-31

Awasthi, A., L. Riol-Blanco, A. Jäger, T. Korn, C. Pot, G. Galileos, E. Bettelli, V.K. Kuchroo, and M. Oukka. 2009. Cutting edge: IL-23 receptor gfp reporter mice reveal distinct populations of IL-17-producing cells. *J. Immunol.* 182:5904–5908. https://doi.org/10.4049/jimmunol.0900732

Barreau, C., F. Bimet, M. Kiredjian, N. Rouillon, and C. Bizet. 1993. Comparative chemotaxonomic studies of mycolic acid-free coryneform bacteria of human origin. *J. Clin. Microbiol.* 31:2085–2090.

Belheouane, M., Y. Gupta, S. Künzel, S. Ibrahim, and J.F. Baines. 2017. Improved detection of gene-microbe interactions in the mouse skin microbiota using high-resolution QTL mapping of 16S rRNA transcripts. *Microbiome.* 5:59. https://doi.org/10.1186/s40168-017-0275-5

Belkaid, Y., and J.A. Segre. 2014. Dialogue between skin microbiota and immunity. *Science.* 346:954–959. https://doi.org/10.1126/science.1260144

Bou Raad, R., X. Méniche, C. de Sousa-d'Auria, M. Chami, C. Salmeron, M. Tropis, C. Labarre, M. Daffé, C. Houssin, and N. Bayan. 2010. A deficiency in arabinogalactan biosynthesis affects Corynebacterium glutamicum mycolate outer membrane stability. *J. Bacteriol.* 192:2691–2700. https://doi.org/10.1128/JB.00009-10

Burkovski, A. 2013. Cell envelope of corynebacteria: Structure and influence on pathogenicity. *ISRN Microbiol.* 2013:935736. https://doi.org/10.1155/2013/935736

Cai, Y., X. Shen, C. Ding, C. Qi, K. Li, X. Li, V.R. Jala, H.G. Zhang, T. Wang, J. Zheng, and J. Yan. 2011. Pivotal role of dermal IL-17-producing γδ T cells in skin inflammation. *Immunity.* 35:596–610. https://doi.org/10.1016/j.immuni.2011.08.001

Conlan, S., L.A. Mijares, J. Becker, R.W. Blakesley, G.G. Bouffard, S. Brooks, H. Coleman, J. Gupta, N. Gurson, M. Park, et al. NISC Comparative Sequencing Program. 2012. Staphylococcus epidermidis pan-genome sequence analysis reveals diversity of skin commensal and hospital infection-associated isolates. *Genome Biol.* 13:R64. https://doi.org/10.1186/gb-2012-13-7-r64

Converse, S.E., and J.S. Cox. 2005. A protein secretion pathway critical for Mycobacterium tuberculosis virulence is conserved and functional in Mycobacterium smegmatis. *J. Bacteriol.* 187:1238–1245. https://doi.org/10.1128/JB.187.4.1238-1245.2005

Dörner, U., B. Schiffler, M.A. Lanéelle, M. Daffé, and R. Benz. 2009. Identification of a cell-wall channel in the corynemycolic acid-free Gram-positive bacterium *Corynebacterium amycolatum*. *Int. Microbiol.* 12:29–38.

Eggeling, L., and M. Bott. 2005. Handbook of *Corynebacterium glutamicum*. Taylor & Francis, Boca Raton, FL. 616 pp.

Gande, R., K.J. Gibson, A.K. Brown, K. Krumbach, L.G. Dover, H. Sahm, S. Shioyama, T. Oikawa, G.S. Besra, and L. Eggeling. 2004. Acyl-CoA carboxylases (accD2 and accD3), together with a unique polyketide synthase (Cg-pks), are key to mycolic acid biosynthesis in Corynebacterianeae such as Corynebacterium glutamicum and Mycobacterium tuberculosis. *J. Biol. Chem.* 279:44847–44857. https://doi.org/10.1074/jbc.M408648200

Gao, Z., C.H. Tseng, B.E. Strober, Z. Pei, and M.J. Blaser. 2008. Substantial alterations of the cutaneous bacterial biota in psoriatic lesions. *PLoS One.* 3:e2719. https://doi.org/10.1371/journal.pone.0002719

Gray, E.E., F. Ramírez-Valle, Y. Xu, S. Wu, Z. Wu, K.E. Karjalainen, and J.G. Cyster. 2013. Deficiency in IL-17-committed Vγ4(+) γδ T cells in a spontaneous Sox13-mutant CD45.1(+) congenic mouse substrain provides protection from dermatitis. *Nat. Immunol.* 14:584–592. https://doi.org/10.1038/ni.2585

Grice, E.A., and J.A. Segre. 2011. The skin microbiome. *Nat. Rev. Microbiol.* 9:244–253. https://doi.org/10.1038/nrmicro2537

Grice, E.A., H.H. Kong, S. Conlan, C.B. Deming, J. Davis, A.C. Young, G.G. Bouffard, R.W. Blakesley, P.R. Murray, E.D. Green, et al. 2009. Topographical and temporal diversity of the human skin microbiome. *Science.* 324:1190–1192. https://doi.org/10.1126/science.1171700

Grice, E.A., E.S. Snitkin, L.J. Yockey, D.M. Bermudez, K.W. Liechty, J.A. Segre; NISC Comparative Sequencing Program. 2010. Longitudinal shift in diabetic wound microbiota correlates with prolonged skin defense response. *Proc. Natl. Acad. Sci. USA.* 107:14799–14804. https://doi.org/10.1073/pnas.1004204107

Ha, H.L., H. Wang, P. Pisitkun, J.C. Kim, I. Tassi, W. Tang, M.I. Morasso, M.C. Udey, and U. Siebenlist. 2014. IL-17 drives psoriatic inflammation via distinct, target cell-specific mechanisms. *Proc. Natl. Acad. Sci. USA.* 111:E3422–E3431. https://doi.org/10.1073/pnas.1400513111

Heilig, J.S., and S. Tonegawa. 1986. Diversity of murine gamma genes and expression in fetal and adult T lymphocytes. *Nature.* 322:836–840. https://doi.org/10.1038/322836a0

Holderness, J., J.F. Hedges, A. Ramstead, and M.A. Jutila. 2013. Comparative biology of γδ T cell function in humans, mice, and domestic animals. *Annu. Rev. Anim. Biosci.* 1:99–124. https://doi.org/10.1146/annurev-animal-031412-103639

Hsu, Y.M., Y. Zhang, Y. You, D. Wang, H. Li, O. Duramad, X.F. Qin, C. Dong, and X. Lin. 2007. The adaptor protein CARD9 is required for innate immune responses to intracellular pathogens. *Nat. Immunol.* 8:198–205. https://doi.org/10.1038/ni1426

Kobayashi, T., M. Glatz, K. Horiuchi, H. Kawasaki, H. Akiyama, D.H. Kaplan, H.H. Kong, M. Amagai, and K. Nagao. 2015. Dysbiosis and *Staphylococcus aureus* colonization drives inflammation in atopic dermatitis. *Immunity.* 42:756–766. https://doi.org/10.1016/j.immuni.2015.03.014

Korf, J., A. Stoltz, J. Verschoor, P. De Baetselier, and J. Grooten. 2005. The *Mycobacterium tuberculosis* cell wall component mycolic acid elicits pathogen-associated host innate immune responses. *Eur. J. Immunol.* 35:890–900. https://doi.org/10.1002/eji.200425332

Kuleshov, M.V., M.R. Jones, A.D. Rouillard, N.F. Fernandez, Q. Duan, Z. Wang, S. Koplev, S.L. Jenkins, K.M. Jagodnik, A. Lachmann, et al. 2016. Enrichr: A comprehensive gene set enrichment analysis web server 2016 update. *Nucleic Acids Res.* 44(W1):W90–W97. https://doi.org/10.1093/nar/gkw377

Lai, Y., A. Di Nardo, T. Nakatsuji, A. Leichtle, Y. Yang, A.L. Cogen, Z.R. Wu, L.V. Hooper, R.R. Schmidt, S. von Aulock, et al. 2009. Commensal bacteria regulate Toll-like receptor 3-dependent inflammation after skin injury. *Nat. Med.* 15:1377–1382. https://doi.org/10.1038/nm.2062

Langowski, J.L., X. Zhang, L. Wu, J.D. Mattson, T. Chen, K. Smith, B. Basham, T. McClanahan, R.A. Kastelein, and M. Oft. 2006. IL-23 promotes tumour incidence and growth. *Nature.* 442:461–465. https://doi.org/10.1038/nature04808

Liang, D., A. Zuo, H. Shao, W.K. Born, R.L. O'Brien, H.J. Kaplan, and D. Sun. 2013. IL-23 receptor expression on γδ T cells correlates with their enhancing or suppressive effects on autoreactive T cells in experimental autoimmune uveitis. *J. Immunol.* 191:1118–1125. https://doi.org/10.4049/jimmunol.1300626

Matsunaga, I., and D.B. Moody. 2009. Mincle is a long sought receptor for mycobacterial cord factor. *J. Exp. Med.* 206:2865–2868. https://doi.org/10.1084/jem.20092533

Minnikin, D.E., I.G. Hutchinson, and A.B. Caldicott. 1980. Thin-layer chromatography of methanolysates of mycolic acid-containing bacteria. *J. Chromatogr. A.* 188:221–233. https://doi.org/10.1016/S0021-9673(00)88433-2

Mishra, A.K., L.J. Alderwick, D. Rittmann, C. Wang, A. Bhatt, W.R. Jacobs Jr., K. Takayama, L. Eggeling, and G.S. Besra. 2008. Identification of a novel alpha(1–>6) mannopyranosyltransferase MptB from *Corynebacterium glutamicum* by deletion of a conserved gene, NCgl1505, affords a lipomannan- and lipoarabinomannan-deficient mutant. *Mol. Microbiol.* 68:1595–1613. https://doi.org/10.1111/j.1365-2958.2008.06265.x

Naik, S., N. Bouladoux, C. Wilhelm, M.J. Molloy, R. Salcedo, W. Kastenmuller, C. Deming, M. Quinones, L. Koo, S. Conlan, et al. 2012. Compartmentalized control of skin immunity by resident commensals. *Science.* 337:1115–1119. https://doi.org/10.1126/science.1225152

Naik, S., N. Bouladoux, J.L. Linehan, S.J. Han, O.J. Harrison, C. Wilhelm, S. Conlan, S. Himmelfarb, A.L. Byrd, C. Deming, et al. 2015. Commensal-dendritic-cell interaction specifies a unique protective skin immune signature. *Nature.* 520:104–108. https://doi.org/10.1038/nature14052

Padhi, T., and Garima. 2013. Metabolic syndrome and skin: psoriasis and beyond. *Indian J. Dermatol.* 58:299–305. https://doi.org/10.4103/0019-5154.113950

Puig, L. 2017. The role of IL 23 in the treatment of psoriasis. *Expert Rev. Clin. Immunol.* 13:525–534. https://doi.org/10.1080/1744666X.2017.1292137

Quan, J., and J. Tian. 2011. Circular polymerase extension cloning for high-throughput cloning of complex and combinatorial DNA libraries. *Nat. Protoc.* 6:242–251. https://doi.org/10.1038/nprot.2010.181

Ramírez-Valle, F., E.E. Gray, and J.G. Cyster. 2015. Inflammation induces dermal Vγ4+ γδT17 memory-like cells that travel to distant skin and accelerate secondary IL-17-driven responses. *Proc. Natl. Acad. Sci. USA.* 112:8046–8051. https://doi.org/10.1073/pnas.1508990112

Riol-Blanco, L., V. Lazarevic, A. Awasthi, M. Mitsdoerffer, B.S. Wilson, A. Croxford, A. Waisman, V.K. Kuchroo, L.H. Glimcher, and M. Oukka. 2010. IL-23 receptor regulates unconventional IL-17-producing T cells that control bacterial infections. *J. Immunol.* 184:1710–1720. https://doi.org/10.4049/jimmunol.0902796

Riol-Blanco, L., J. Ordovas-Montanes, M. Perro, E. Naval, A. Thiriot, D. Alvarez, S. Paust, J.N. Wood, and U.H. von Andrian. 2014. Nociceptive sensory neurons drive interleukin-23-mediated psoriasiform skin inflammation. *Nature.* 510:157–161. https://doi.org/10.1038/nature13199

Scharschmidt, T.C., and M.A. Fischbach. 2013. What lives on our skin: Ecology, genomics and therapeutic opportunities of the skin microbiome. *Drug Discov. Today Dis. Mech.* 10:e83–89. https://doi.org/10.1016/j.ddmec.2012.12.003

Sutton, C.E., S.J. Lalor, C.M. Sweeney, C.F. Brereton, E.C. Lavelle, and K.H. Mills. 2009. Interleukin-1 and IL-23 induce innate IL-17 production from gammadelta T cells, amplifying Th17 responses and autoimmunity. *Immunity.* 31:331–341. https://doi.org/10.1016/j.immuni.2009.08.001

Vantourout, P., and A. Hayday. 2013. Six-of-the-best: Unique contributions of γδ T cells to immunology. *Nat. Rev. Immunol.* 13:88–100. https://doi.org/10.1038/nri3384

Wang, K., and M. Karin. 2015. The IL-23 to IL-17 cascade inflammation-related cancers. *Clin. Exp. Rheumatol.* 33(4, Suppl 92):S87–S90.

Yamasaki, S., M. Matsumoto, O. Takeuchi, T. Matsuzawa, E. Ishikawa, M. Sakuma, H. Tateno, J. Uno, J. Hirabayashi, Y. Mikami, et al. 2009. C-type lectin Mincle is an activating receptor for pathogenic fungus, Malassezia. *Proc. Natl. Acad. Sci. USA.* 106:1897–1902. https://doi.org/10.1073/pnas.0805177106

Zhang, Y., Q. Li, E. Rao, Y. Sun, M.E. Grossmann, R.J. Morris, M.P. Cleary, and B. Li. 2015. Epidermal fatty acid binding protein promotes skin inflammation induced by high-fat diet. *Immunity.* 42:953–964. https://doi.org/10.1016/j.immuni.2015.04.016